Supplement of Atmos. Chem. Phys., 19, 10205–10216, 2019
https://doi.org/10.5194/acp-19-10205-2019-supplement

Atmospheric Chemistry and Physics
Open Access
EGU

Supplement of

Summertime aerosol volatility measurements in Beijing, China

Weiqi Xu et al.

Correspondence to: Yele Sun (sunyele@mail.iap.ac.cn)

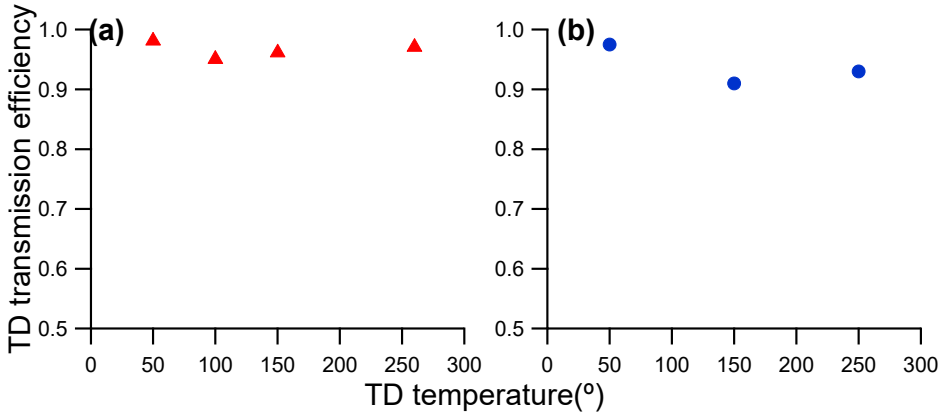

Figure S1. Particle mass loss within the thermal denuder in summer of (a) 2017 and (b) 2018.

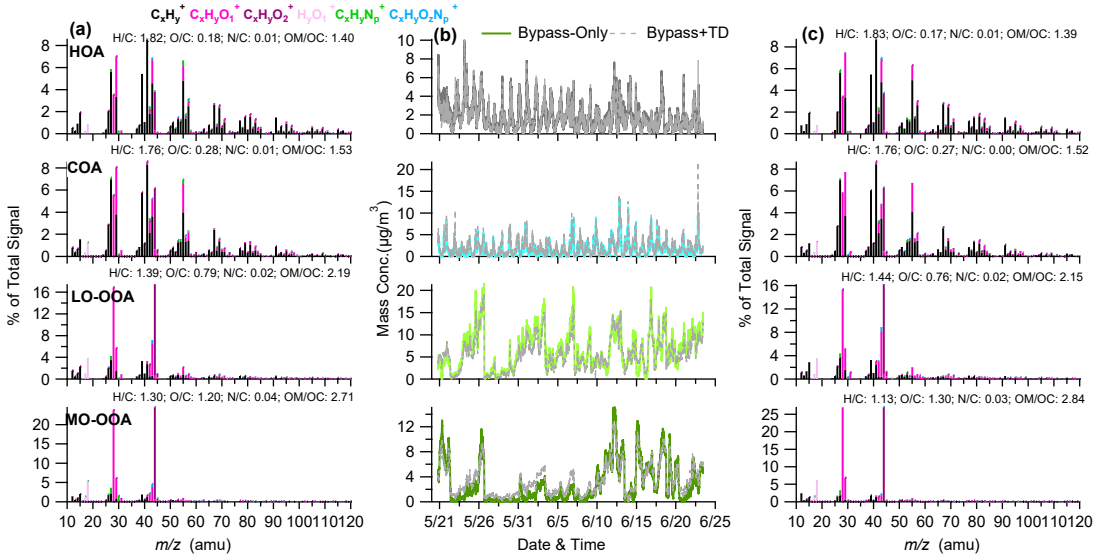

Figure S2. Mass spectra of OA factor resolved by (a) $MS_{ambient}$ and (c) $MS_{ambient+TD}$ using ME-2 analysis. (b) shows a comparison of time series of OA factor resolved from $MS_{ambient}$ and $MS_{ambient+TD}$ in summer 2018.

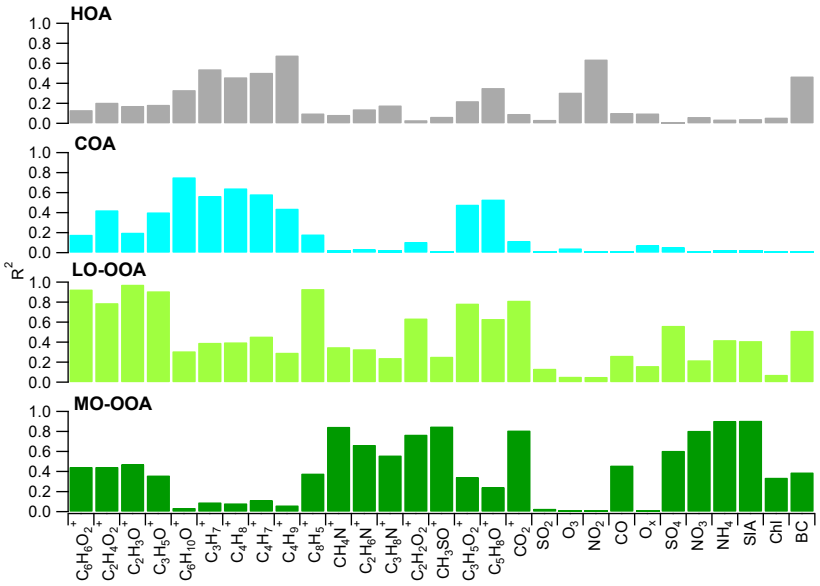

Figure S3. Correlation between OA factors and tracers in summer 2018.

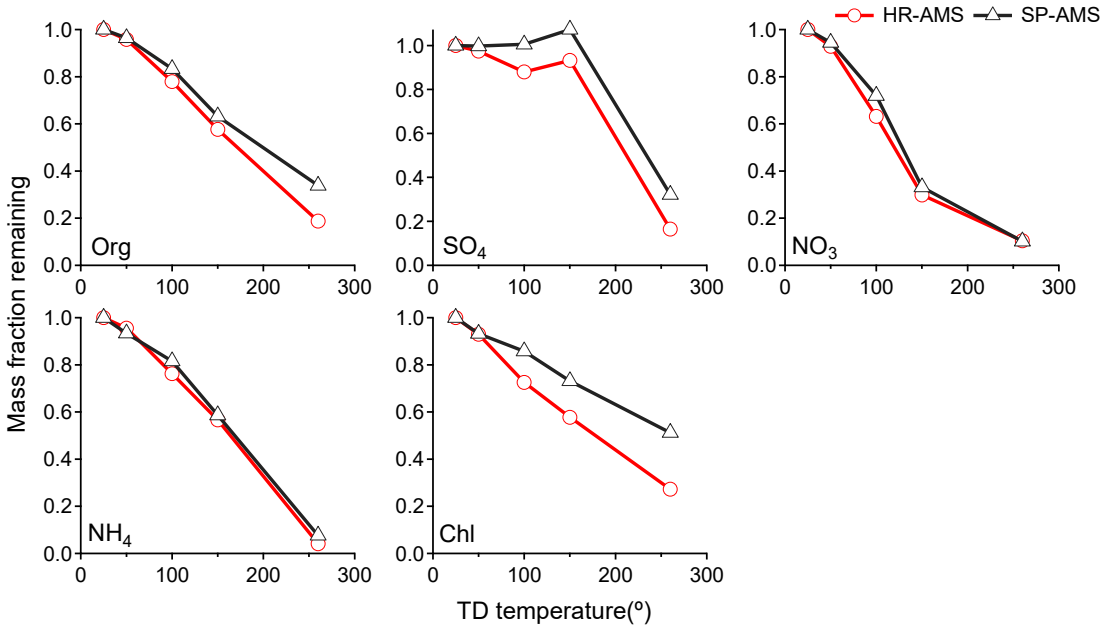

Figure S4. Thermograms of aerosol species measured by TD-HR-AMS and TD-SP-AMS in 2017.

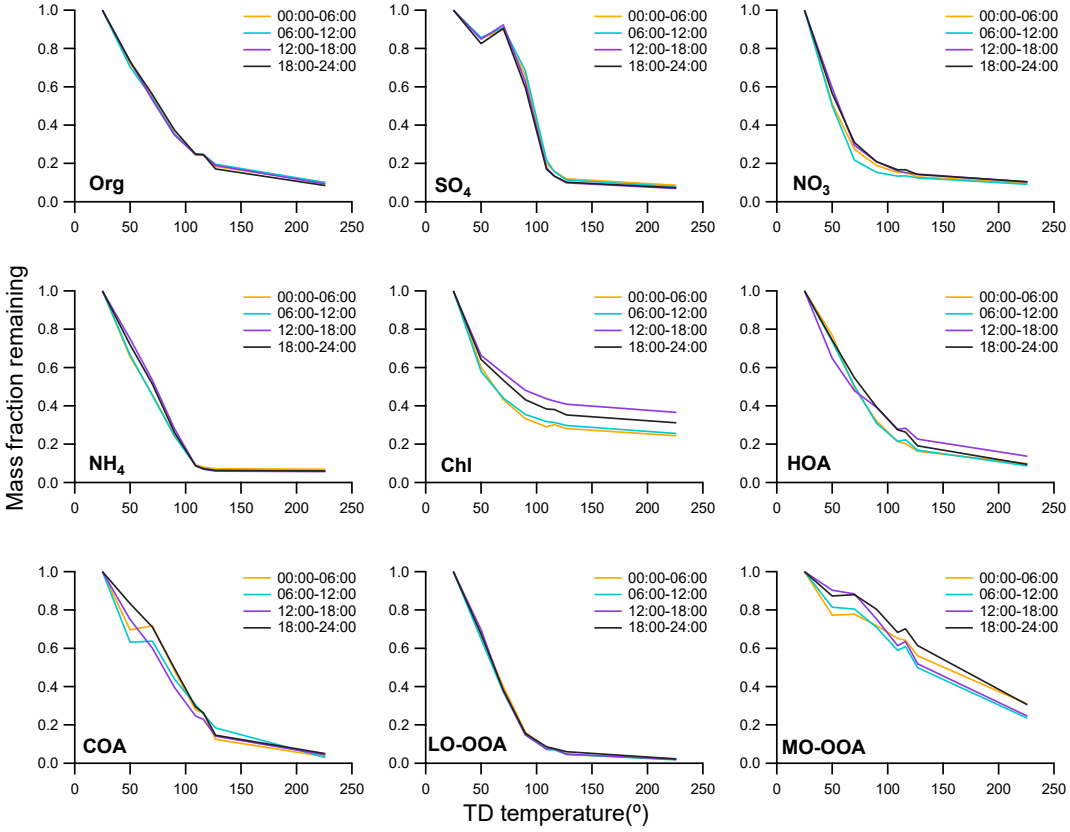

Figure S5. Thermograms of aerosol species and OA factors during four different time periods in 2018.

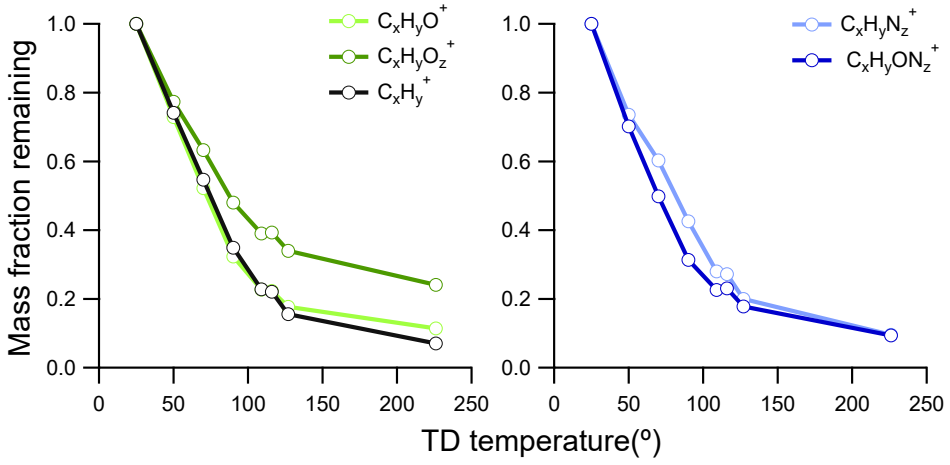

Figure S6. Thermograms of four different ion families in summer 2018.

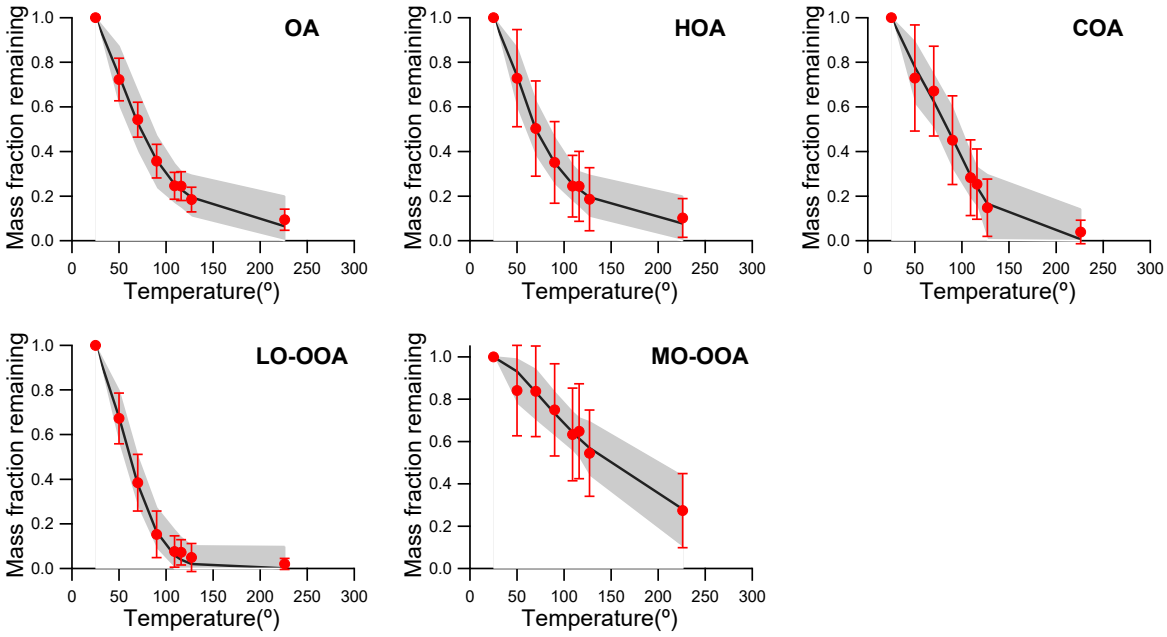

Figure S7. Thermograms of OA and OA factors measured by TD-HR-AMS in 2018. The solid circles represent the measurements and the error bars are one standard deviation. The black lines refer to the best-predicted MFR using the algorithm of Karnezi et al. (2014)

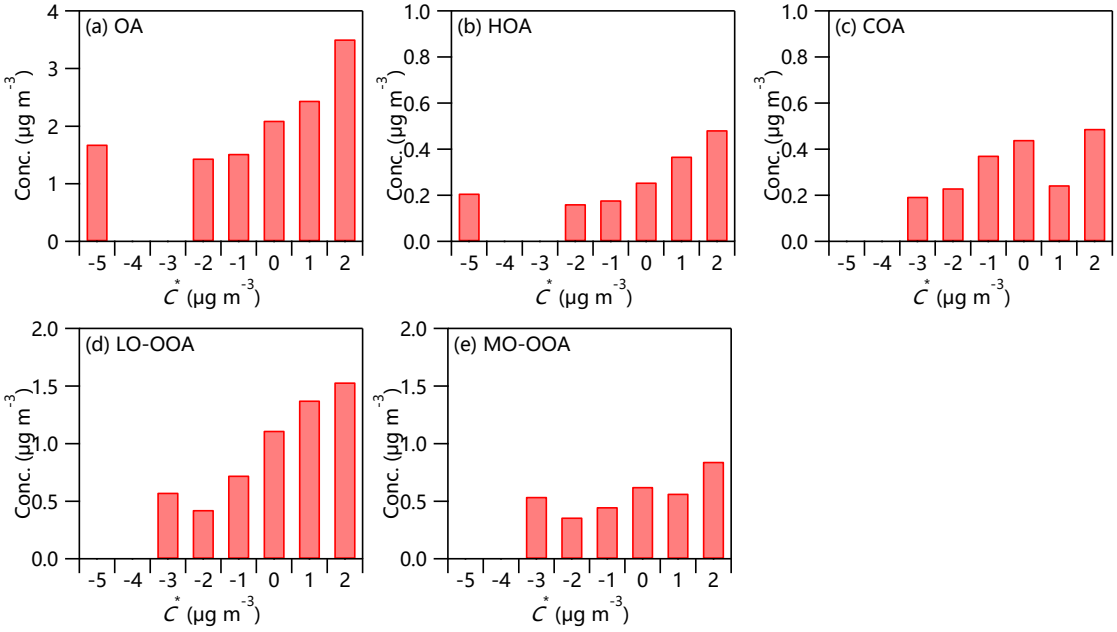

Figure S8. Predicted absolute OA and four OA factors concentrations at different volatility bins in 2018.

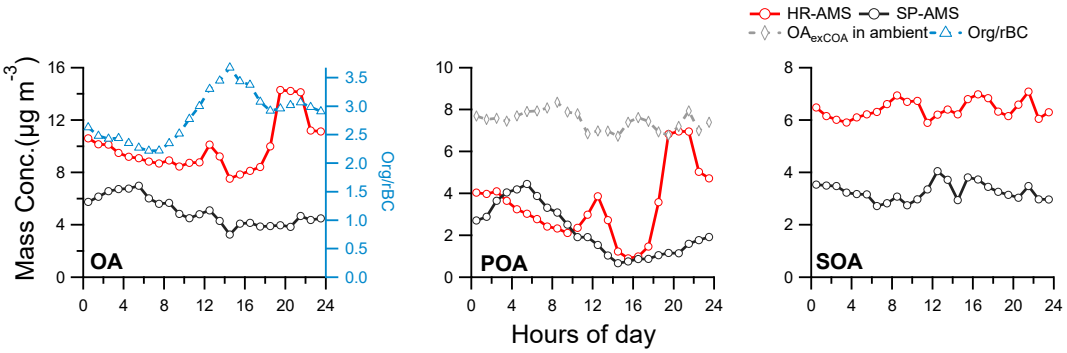

Figure S9. Average diurnal cycles of Org/rBC ratio, and mass concentrations of ambient and BC-containing OA, POA and SOA.

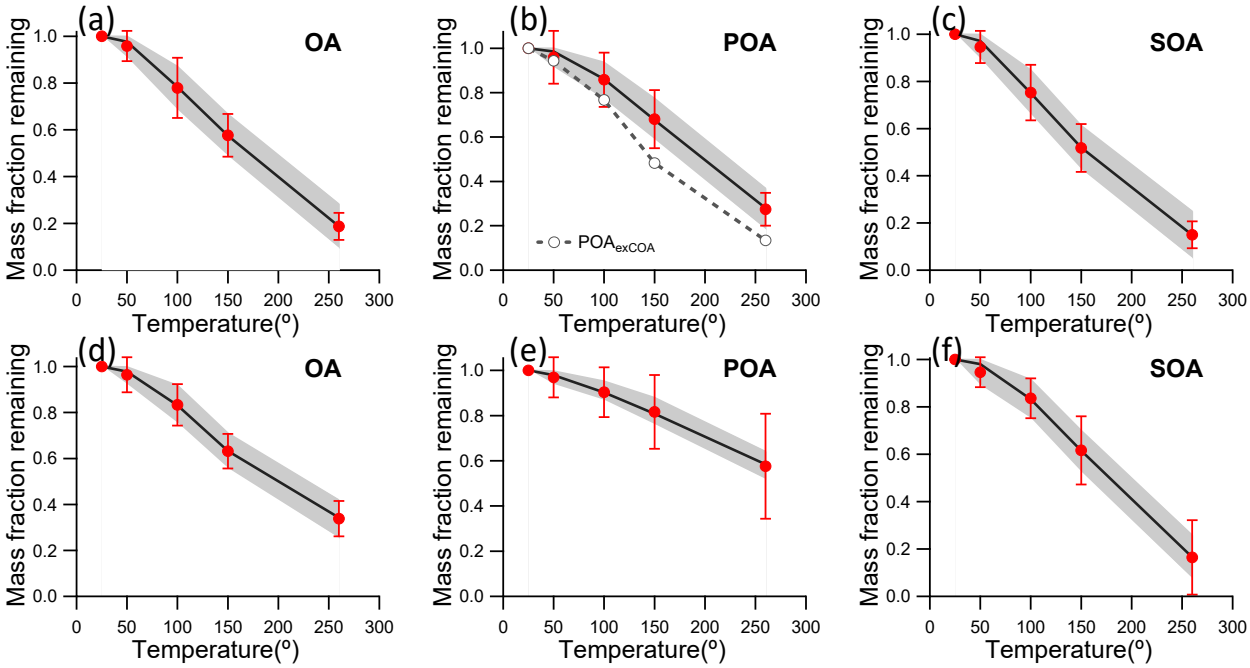

Figure S10. Thermograms of OA, POA and SOA factors measured by (a,b,c) TD-HR-AMS and (d,e,f) TD-SP-AMS in 2017. The solid circles represent the measurements, and the error bars are one standard deviation. The black lines refer to the best-predicted MFR using the algorithm of Karnezi et al. (2014)

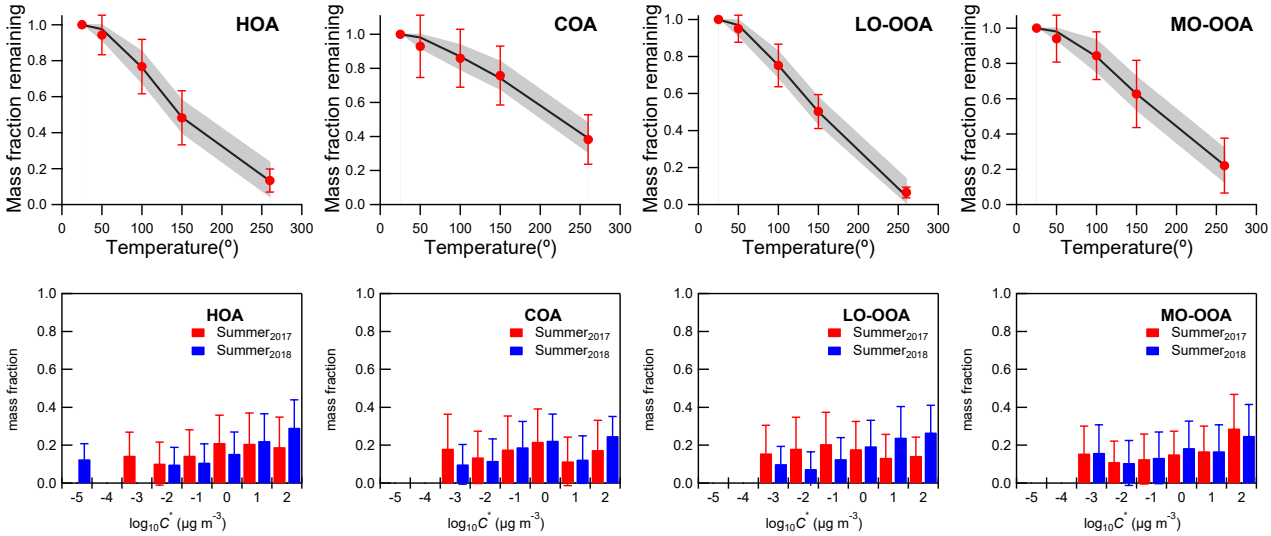

Figure S11. Thermograms and predicted volatility distributions of four OA factors measured by TD-HR-AMS in 2017. The solid circles represent the measurements and the error bars are one standard deviation. The black lines refer to the best-predicted MFR using the algorithm of Karnezi et al. (2014). The error bars in bottom panels are the uncertainties derived using the approach of Karnezi et al. (2014). Predicted volatility distributions of four OA factors in 2018 are also shown for comparisons.

Table S1. Average ambient concentrations, threshold concentrations for PM species and OA factors and corresponding fraction of the data above the threshold.

	Average mass concentration ($\mu g\ m^{-3}$)	Threshold concentration ($\mu g\ m^{-3}$)	% of measurements above threshold
$HR\text{-}AMS_{2018}$			
Org	12.7	1.5	99.6%
SO_4	6.5	0.4	99.7%
NO_3	7.4	0.06	99.6%
NH_4	4.3	0.16	99.6%
Chl	0.18	0.02	98.6%
HOA	1.7	0.05	97.6%
COA	2.0	0.04	97.6%
LO-OOA	5.8	0.4	97.2%
MO-OOA	3.4	0.5	98.5%
$HR\text{-}AMS_{2017}$			
Org	9.8	2.98	97.6%
POA	3.4	0.48	99.5%
HOA	1.0	0.19	98.9%
COA	2.4	0.16	96.4%
SOA	6.4	1.31	98.2%
LO-OOA	3.8	1.01	97.6%
MO-OOA	2.6	0.12	98.6%
$SP\text{-}AMS_{2017}$			
Org	5.5	1.3	98.6%
POA	2.2	0.41	96.7%
SOA	3.3	0.81	97.7%

Table S2. Average peak diameters of SOA and POA in summer of 2017 and 2018.

	Average peak diameters (nm)
$HR\text{-}AMS_{2018}$	
OA	536
POA	485
SOA	600
$HR\text{-}AMS_{2017}$	
OA	371
POA	350
SOA	380
$SP\text{-}AMS_{2017}$	
OA	235
POA	150
SOA	298

Table S3. Best fit OA volatility parameter values in previous field studies.

Species	Volatility distribution											ΔH	a_m
	10^{-8}	10^{-7}	10^{-6}	10^{-5}	10^{-4}	10^{-3}	10^{-2}	10^{-1}	10^{0}	10^{1}	10^{2}		
OA[a]						0.2	0.2	0.3	0.3			80	1
OA[a]							0.2	0.2	0.3	0.3		80	0.05
HOA[b]					0.13	0.14	0.08	0.02	0.06	0.57		100	1
COA[b]				0.13	0.15	0.07	0.2	0.08	0.37			100	1
MOA[b]					0.03	0.03	0.05	0.28	0.42	0.19		100	1
SV-OOA[b]					0.06	0.14	0.15	0.13	0.18	0.34		100	1
LV-OOA[b]		0.2	0.24	0.28	0.25	0.03						100	1
HOA[c]					0.11	0.09	0.07	0.12	0.11	0.5		100	1
COA[c]			0.12	0.11	0.14	0.42	0.11	0.1				100	1
BBOA[c]					0.2	0.09	0.08	0.13	0.09	0.41		100	1
OOA[c]					0.3	0.09	0.07	0.09	0.1	0.35		100	1
OA[d]	0.3					0.08	0.12	0.12	0.12	0.26		100	1
OOA[d]	0.41					0.11	0.09	0.08	0.11	0.2		100	1
HOA[d]	0.3					0.07	0.14	0.21	0.17	0.11		100	1
BBOA[d]	0.1					0.1	0.15	0.15	0.14	0.36		100	1
COA[d]	0.1					0.52	0.08	0.05	0.07	0.18		100	1
OA[e]					0.14	0.05	0.06	0.15	0.29	0.31		100	0.5
OA[f]					0.14	0.06	0.08	0.12	0.28	0.32		100	0.5
MO-OOA[g]								0.44	0.14	0.42		89	1
LO-OOA[g]								0.27	0.19	0.54		58	1
isoprene-OA[g]								0.41	0.16	0.43		63	1
BBOA[g]								0.47	0.29	0.24		55	1
OA[g]								0.54	0.19	0.27		86	1
OA[h]			0.06	0.06	0.06	0.07	0.07	0.08	0.10	0.16	0.34	100	1
OA[h]					0.27	0.11	0.11	0.12	0.15	0.24		100	1
OA[h]			0.04	0.04	0.04	0.04	0.05	0.06	0.1	0.2	0.43	100	0.1
OA[h]					0.21	0.07	0.09	0.10	0.18	0.35		100	0.1

[a] Sampling site is Finokalia, and the sampling time is May, 2008. (Lee et al., 2010). This estimation use the transfer model of Riipinen et al. (2010) with least-squares minimization. Assumed a priori values for the effective vaporization enthalpy with 80 KJ mol^{-1} and the mass accommodation coefficient with 1/0.05.

[b and C] Sampling site is Paris, and the sampling time is July, 2009 and January/February 2010, respectively(Paciga et al., 2016). This estimation use the transfer model of Riipinen et al. (2010), and the uncertainties are calculated by Karnezi et al. (2014). Assumed a priori values for the effective vaporization enthalpy with 100 KJ mol^{-1} and the mass accommodation coefficient with 1.

[d] Sampling site is Athens, and the sampling time is January/February 2013 (Louvaris et al., 2017). This estimation use the transfer model

of Riipinen et al. (2010), and the uncertainties are calculated by Karnezi et al. (2014). Assumed a priori values for the effective vaporization enthalpy with 100 KJ mol^{-1} and the mass accommodation coefficient with 1.

[e and f] Sampling site is Centreville and Raleigh, and the sampling time is June/July and Nov./Oct. 2013, respectively (Saha et al., 2017). This estimation use the volatility parameter extraction framework(Saha et al., 2015) to extract a set of volatility parameter (C^*, Hvap, γe) values via inversion of dual-TD data using an evaporation kinetics model.

[g] Sampling site is Centreville, and the sampling time is June/July 2013 (Kostenidou et al., 2018). This estimation use the transfer model of Riipinen et al. (2010), and the uncertainties are calculated by Karnezi et al. (2014). The enthalpy of vaporization was also estimated, while the accommodation coefficient was assumed to be equal to unity.

[h] Sampling site is Mexico City, and the sampling time is March/April 2006(Cappa and Jimenez, 2010)

References

Cappa, C. D., and Jimenez, J. L.: Quantitative estimates of the volatility of ambient organic aerosol, Atmos. Chem. Phys., 10, 5409-5424, 10.5194/acp-10-5409-2010, 2010.

Karnezi, E., Riipinen, I., and Pandis, S. N.: Measuring the atmospheric organic aerosol volatility distribution: a theoretical analysis, Atmospheric Measurement Techniques, 7, 2953-2965, 10.5194/amt-7-2953-2014, 2014.

Kostenidou, E., Karnezi, E., Hite Jr, J. R., Bougiatioti, A., Cerully, K., Xu, L., Ng, N. L., Nenes, A., and Pandis, S. N.: Organic aerosol in the summertime southeastern United States: components and their link to volatility distribution, oxidation state and hygroscopicity, Atmos. Chem. Phys., 18, 5799-5819, 10.5194/acp-18-5799-2018, 2018.

Lee, B. H., Kostenidou, E., Hildebrandt, L., Riipinen, I., Engelhart, G. J., Mohr, C., DeCarlo, P. F., Mihalopoulos, N., Prevot, A. S. H., Baltensperger, U., and Pandis, S. N.: Measurement of the ambient organic aerosol volatility distribution: application during the Finokalia Aerosol Measurement Experiment (FAME-2008), Atmos. Chem. Phys., 10, 12149-12160, 10.5194/acp-10-12149-2010, 2010.

Louvaris, E. E., Florou, K., Karnezi, E., Papanastasiou, D. K., Gkatzelis, G. I., and Pandis, S. N.: Volatility of source apportioned wintertime organic aerosol in the city of Athens, Atmos. Environ., 158, 138-147, 10.1016/j.atmosenv.2017.03.042, 2017.

Paciga, A., Karnezi, E., Kostenidou, E., Hildebrandt, L., Psichoudaki, M., Engelhart, G. J., Lee, B.-H., Crippa, M., Prevot, A. S. H., Baltensperger, U., and Pandis, S. N.: Volatility of organic aerosol and its components in the megacity of Paris, Atmos. Chem. Phys., 16, 2013-2023, 10.5194/acp-16-2013-2016, 2016.

Riipinen, I., Pierce, J. R., Donahue, N. M., and Pandis, S. N.: Equilibration time scales of organic aerosol inside thermodenuders: Evaporation kinetics versus thermodynamics, Atmos. Environ., 44, 597-607, 10.1016/j.atmosenv.2009.11.022, 2010.

Saha, P. K., Khlystov, A., and Grieshop, A. P.: Determining Aerosol Volatility Parameters Using a “Dual Thermodenuder” System: Application to Laboratory-Generated Organic Aerosols, Aerosol Sci. Tech., 49, 620-632, 10.1080/02786826.2015.1056769, 2015.

Saha, P. K., Khlystov, A., Yahya, K., Zhang, Y., Xu, L., Ng, N. L., and Grieshop, A. P.: Quantifying the volatility of organic aerosol in the southeastern US, Atmos. Chem. Phys., 17, 501-520, 10.5194/acp-17-501-2017, 2017.